A new methanol solvate and Hirshfeld analysis of π-stacking in 2,3,6,7,10,11-hexahydroxytriphenylene solvates

Anirban Karmakar, Ana E. Platero-Prats and Lars Öhrström

Crystallography Journals Online is available from **journals.iucr.org**

A new methanol solvate and Hirshfeld analysis of π-stacking in 2,3,6,7,10,11-hexahydroxytriphenylene solvates

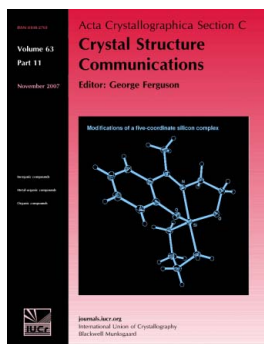Anirban Karmakar,[a] Ana E. Platero-Prats[b] and Lars Öhrström[a]*

[a]Department of Chemical and Biological Engineering, Chalmers University of Technology, SE-412 96 Göteborg, Sweden, and [b]Department of Materials and Environmental Chemistry (MMK), Stockholm University, Sweden
Correspondence e-mail: ohrstrom@chalmers.se

The structure of 2,3,6,7,10,11-hexahydroxytriphenylene (hhtp) methanol monosolvate, $C_{18}H_{12}O_6 \cdot CH_3OH$, has triclinic symmetry (space group $P\bar{1}$). The compound has a three-dimensional layered network structure formed by inter-molecular hydrogen bonding. Structure analysis with Hirsh-feld surfaces is shown to be a sensitive method for comparing π-stacking effects in the five known solvates of hhtp. The title structure shows slightly weaker π-stacking than the dihydrate, but stronger π-stacking than the other three solvates.

Comment

2,3,6,7,10,11-Hexahydroxytriphenylene (hhtp) continues to be important both as a starting material for forming discrete supramolecular units and in its own right (Fyfe *et al.*, 2000; Waldvogel *et al.*, 2000; Bomkamp *et al.*, 2007; Cote *et al.*, 2005; El-Kaderi *et al.*, 2007; Kocyigit *et al.*, 2010; Kocyigit & Guler, 2011; Spitler *et al.*, 2011; Simonsen, 2010). Thus, reporting new polymorphs or solvates is important as these can then be rapidly detected by powder X-ray diffraction. We report here the isolation of a new methanol solvate of hhtp, the title compound, (I), obtained from an unsuccessful reaction of hhtp, pyrazole and trimethyl borate, a reaction used for the purpose of constructing new covalent organic frameworks.

The crystal structure of (I) is distinctly different from those of the other four solvates reported for this compound, *viz.* the monohydrate, (II) [space group $P2_1/c$, $a = 11.127$ (2) Å, $b = 12.797$ (3) Å, $c = 11.081$ (2) Å and $\beta = 119.32$ (3)°; Andresen *et al.*, 2000], the cyclopentanone trisolvate, (III) [space group $P2_1$, $a = 7.986$ (3) Å, $b = 10.161$ (2) Å, $c = 18.554$ (2) Å and $\beta = 99.84$ (1)°], the cyclopentanone tetrasolvate monohydrate, (IV) [space group $P2_1/c$, $a = 7.603$ (7) Å, $b = 20.937$ (3) Å, $c = 22.245$ (3) Å and $\beta = 91.85$ (3)°; Toda *et al.*, 2000], and the dihydrate, (V) [space group *Pbcn*, $a = 14.2694$ (8) Å, $b = 16.5639$ (8) Å, $c = 7.2237$ (4) Å; Thébault *et al.*, 2011].

Methanol solvate (I), in contrast with dihydrate (V), is not stable during extended storage due to loss of crystallinity, explaining the somewhat lower than expected quality of the data.

(I)
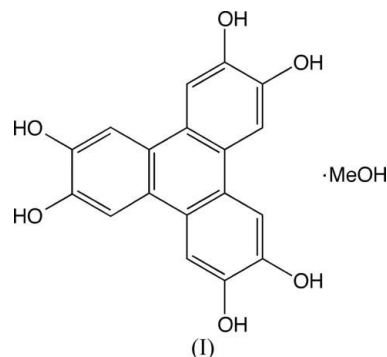
The structure of (I) has a hhtp unit very similar to those in the four previously reported structures (Fig. 1). It is important to check this, as there are some indications that radical species may form (Grange *et al.*, 2010).

The hydrogen-bond networks in (I)–(V) are, to a greater or lesser extent, responsible for the overall structures. Diols of rigid hydrocarbon skeletons are well known to give three-dimensional networks of different topologies (Wells, 1954; Wallentin *et al.*, 2009, 2012), but solvated species may be less obvious to interpret in this way, and the large number of hydroxy groups in the present structure makes this even more difficult. Analyzing the previous four structures, we find that in cyclopentanone solvates (III) and (IV), each hhtp molecule forms hydrogen bonds to four other units, forming a (4,4)-connected two-dimensional network, with the cyclopentanone molecules hydrogen bonded and protruding from the network and with a layer of cyclopentanone molecules effectively isolating the flat parts of the aromatic skeletons from each
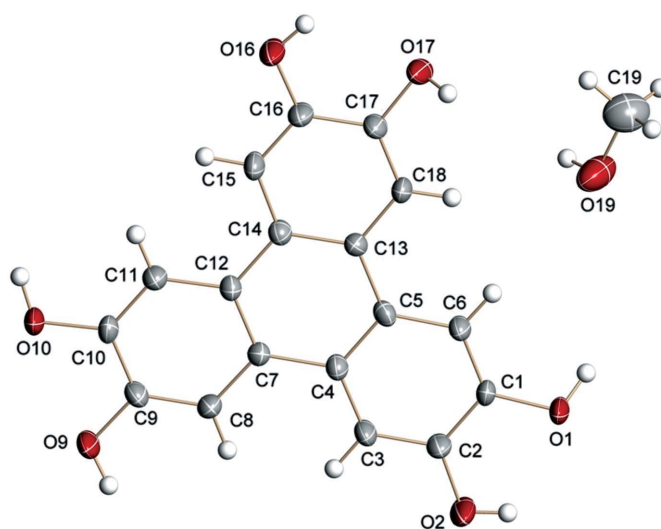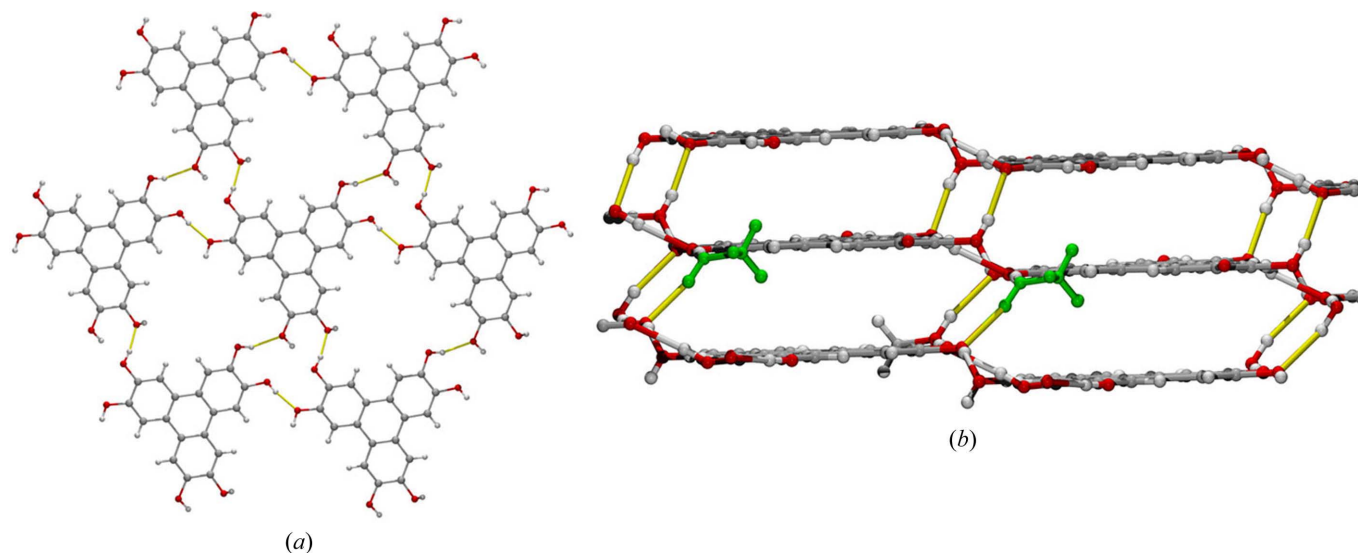

Figure 1
The asymmetric unit of (I), showing the atom-numbering scheme. Displacement ellipsoids are drawn at the 50% probability level.

Figure 2
(*a*) The hexagonal layer built by hydrogen bonding between hhtp molecules. (*b*) The inter-layer hydrogen bonding implied in the formation of the final three-dimensional structure. Hydrogen bonds are shown as lighter lines.

other. In monohydrate (II), each hhtp molecule forms hydrogen bonds to six other hhtp molecules, giving an intricate double layer of two (4,4) networks where each vertex connects to two other vertices in the neighbouring network. The water molecules connect these layers into a complicated three-dimensional network through hydrogen bonding, and in dihydrate (V) the (4,4) two-dimensional network seen in (III) and (IV) is reproduced and further crosslinked by water molecules to form a complex three-dimensional network.

In (I), hexagonal hydrogen-bonded two-dimensional layers are formed with parallel but slightly twisted hhtp molecules. One hhtp molecule interconnects with six neighbouring hhtp molecules *via* hydrogen bonds. These layers are further connected by one hydrogen bond per hhtp molecule to the closest layer (O17—H17A···O1^{ii}, Table 1), giving a two-layer structure (Fig. 2*b*). These double layers are then further connected into an intricate three-dimensional network by hydrogen bonds to methanol molecules (O19—H19···O9^{vi}, Table 1), only slightly protruding from the plane and with their methyl groups in the open spaces in the hexagonal layer. The interpretation of this network in terms of topology would result in a net with at least four different types of vertices, and we do not see any advantage in this type of exercise for understanding or communicating this structure.

The structure of (I) contains two similar interlayer distances and we would expect substantial π–π stacking, as the hydrogen bonds between any type of layer are few. Moreover, the five different structures give us the opportunity to compare the π–π stacking. This comparison will be made using Hirshfeld surfaces (McKinnon *et al.*, 2004).

To calculate the Hirshfeld surfaces one starts by replacing every atom with a spherically averaged theoretical electron density. The surface is then generated by those points at which the calculated electron density from the chosen molecule equals that from the surrounding molecules in the crystal

structure. Inside this surface we now have the volume of the crystal structure wherein the electron density is dominated by the chosen molecule.

The best indicator of π–π stacking on Hirshfeld surfaces is obtained by plotting the shape index. The shape index at a point on the surface is derived from the normal to the surface and the gradient of the surface in two principal directions perpendicular to the normal. For these two directions, the κ_1 and κ_2 values, which represent how much and in which direction the surface is changing, are generated and then used to compute the shape index as $S = (2/\pi)\arctan[(\kappa_1 + \kappa_2)/(\kappa_1 - \kappa_2)]$ (McKinnon *et al.*, 2004). McKinnon and co-workers further noted that this generates complementary surfaces with different signs (usually drawn in red or blue) on two surfaces that touch each other and that the triangular shapes are especially indicative of π–π stacking.

We found that a striking visual comparison could be made by plotting the shape index only for the regions on the surface with close C···C interactions (these generally fall in the region 3.3–3.9 Å). The plots for solvates (I)–(V) are shown in Fig. 3, presented in decreasing order of π–π stacking strength.

In view of the solvent layers separating cyclopentanone solvates (III) and (IV), we do not expect significant π–π stacking in these structures, and indeed the C···C interactions form only 0.4–0.5% of the surface area, the surface itself is clearly nonplanar and the shape index showing only C···C interactions is very small. In contrast, the hydrates and the methanol solvate all show significant π–π stacking, with 12–15% C···C interactions on the surface and striking areas of C···C-filtered shape-index plots. For the monohydrate in particular, the difference between the two sides of the hhtp molecules is clearly shown.

In contrast with the marked differences in π–π stacking, the hydrogen bonding of the hhtp molecule varies only slightly in the five solvates. The hhtp O···H interactions account for 36%
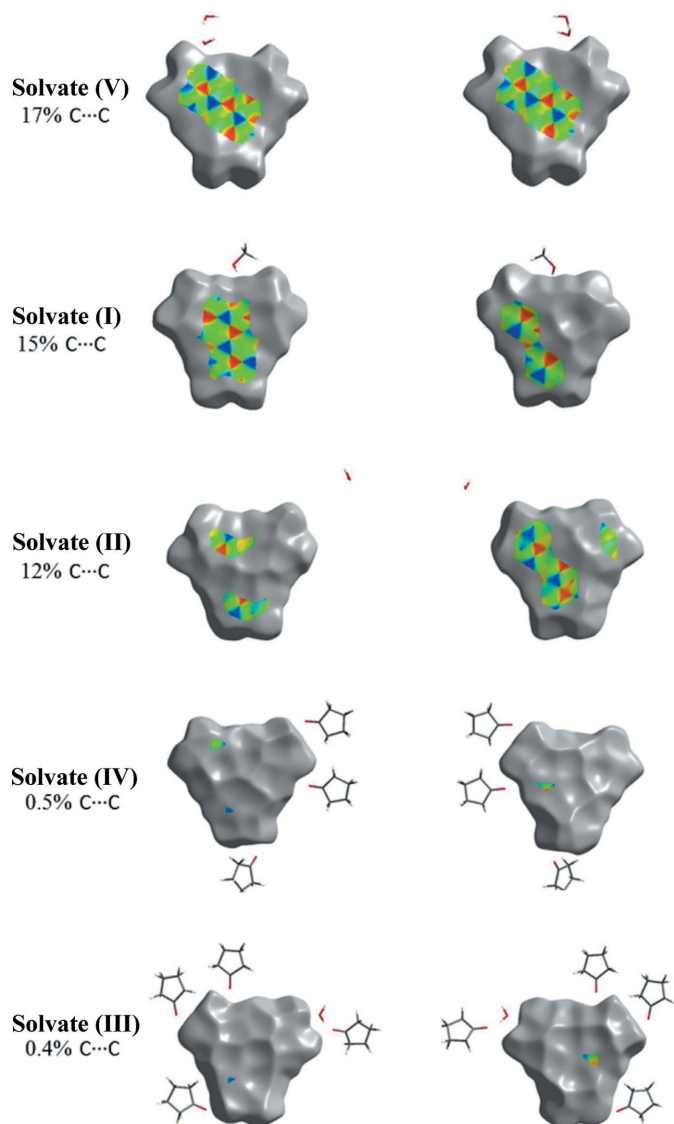
Figure 3
Hirshfeld surfaces with shape indexes, plotted for C···C interactions on both sides of the hhtp molecule for the five differerent solvates, *i.e.* (I)–(V); see *Comment* for full details.

of the hhtp Hirshfeld surface in (I), 35% in (II), 40% in (II), 37% in (IV) and 39% in (V).

Experimental

2,3,6,7,10,11-Hexamethoxytriphenylene (hhtp) was prepared according to the literature method of Zniber *et al.* (2002). Other chemicals were purchased from Aldrich and used as received. X-ray diffraction data collection was performed at the University of Stockholm.

Hhtp (81 mg, 0.25 mmol) and pyrazole (34 mg, 0.5 mmol) were placed in a round-bottomed flask and dissolved in dry CH_3CN (10 ml). To this mixture, a solution of trimethyl borate (52 mg, 0.5 mmol) in dry CH_3CN was added dropwise with continuous stirring. The reaction mixture was stirred for 1 h and a white solid was obtained. The solid product was filtered, washed with acetonitrile and dried in air. The isolated product was dissolved in methanol and colourless crystals of (I) were obtained after 2 d.

Table 1
Hydrogen-bond geometry (Å, °).

D—H···A	D—H	H···A	D···A	D—H···A
O16—H16A···O17	0.84 (3)	2.35 (3)	2.741 (3)	109 (2)
O9—H9A···O17^i	0.85 (3)	1.96 (3)	2.761 (3)	158 (3)
O17—H17A···O1^{ii}	0.81 (4)	1.93 (4)	2.729 (3)	170 (3)
O10—H10A···O19^{iii}	0.86 (3)	1.81 (3)	2.655 (3)	168 (3)
O2—H2A···O1	0.79 (3)	2.29 (3)	2.734 (3)	116 (3)
O2—H2A···O16^{iv}	0.79 (3)	2.00 (3)	2.756 (2)	159 (3)
O1—H1A···O10^v	0.83 (3)	1.90 (3)	2.724 (3)	172 (3)
O19—H19···O9^{vi}	0.82 (4)	2.14 (4)	2.939 (3)	164 (4)

Symmetry codes: (i) $x, y + 1, z - 1$; (ii) $-x + 1, -y + 1, -z + 1$; (iii) $x + 1, y, z - 1$; (iv) $x - 1, y + 1, z$; (v) $x - 1, y, z + 1$; (vi) $-x + 1, -y + 1, -z$.

Crystal data

$C_{18}H_{12}O_6 \cdot CH_4O$	$\gamma = 77.782\ (9)°$
$M_r = 356.32$	$V = 758.6\ (2)$ Å^3
Triclinic, $P\bar{1}$	$Z = 2$
$a = 7.5894\ (7)$ Å	Mo $K\alpha$ radiation
$b = 10.550\ (1)$ Å	$\mu = 0.12$ mm^{-1}
$c = 11.238\ (2)$ Å	$T = 293$ K
$\alpha = 62.88\ (1)°$	$0.15 \times 0.10 \times 0.10$ mm
$\beta = 71.89\ (1)°$	

Data collection

Agilent Xcalibur Sapphire3 diffractometer	2683 independent reflections
4609 measured reflections	1613 reflections with $I > 2\sigma(I)$
	$R_{int} = 0.032$

Refinement

$R[F^2 > 2\sigma(F^2)] = 0.053$	H atoms treated by a mixture of independent and constrained refinement
$wR(F^2) = 0.114$	
$S = 0.97$	
2673 reflections	$\Delta\rho_{max} = 0.22$ e Å^{-3}
255 parameters	$\Delta\rho_{min} = -0.24$ e Å^{-3}

The hydroxy H atoms of htpp were located in a difference Fourier map, their coordinates were freely refined but their displacement parameters were constrained to ride on their parent atoms, with $U_{iso}(H) = 1.5U_{eq}(O)$. Aromatic H atoms were positioned geometrically and were constrained to ride on their parent atoms, with $U_{iso}(H) = 1.2U_{eq}(C)$. Finally, all methanol H atoms were positioned geometrically. Finally, all methanol H atoms were positioned geometrically and constrained to ride on their parent atoms, with $U_{iso}(H) = 1.5U_{eq}(C,O)$.

Data collection: *CrysAlis PRO* (Agilent, 2011); cell refinement: *CrysAlis PRO*; data reduction: *CrysAlis PRO*; program(s) used to solve structure: *SHELXS97* (Sheldrick, 2008); program(s) used to refine structure: *SHELXL97* (Sheldrick, 2008); molecular graphics: *TOPOS* (Blatov *et al.*, 2000) and *CrystalExplorer* (McKinnon *et al.*, 2004); software used to prepare material for publication: *publCIF* (Westrip, 2010).

Supplementary data for this paper are available from the IUCr electronic archives (Reference: CU3018). Services for accessing these data are described at the back of the journal.

organic compounds

References

Agilent (2011). *CrysAlis PRO*. Agilent Technologies, Yarnton, Oxfordshire, England.

Andresen, T. L., Krebs, F. C., Thorup, N. & Bechgaard, K. (2000). *Chem. Mater.* **12**, 2428–2433.

Blatov, V. A., Shevchenko, A. P. & Serezhkin, V. N. (2000). *J. Appl. Cryst.* **33**, 1193.

Bomkamp, M., Siering, C., Landrock, K., Stephan, M., Fröhlich, R. & Waldvogel, S. R. (2007). *Chem. Eur. J.* **13**, 3724–3732.

Cote, A. P., Benin, A. I., Ockwig, N. W., O'Keffee, M., Matzger, A. J. & Yaghi, O. M. (2005). *Science*, **310**, 1166–1170.

El-Kaderi, H. M., Hunt, J. R., Mendoza-Cortes, J. L., Cote, A. P., Taylor, R. E., O'Keefe, M. & Yaghi, O. M. (2007). *Science*, **316**, 268–272.

Fyfe, M. C. T., Lowe, J. N., Stoddart, J. F. & Williams, D. J. (2000). *Org. Lett.* **2**, 1221–1224.

Grange, C. S., Meijer, A. J. H. M. & Ward, M. D. (2010). *Dalton Trans.* **39**, 200–211.

Kocyigit, O. & Guler, E. (2011). *J. Organomet. Chem.* **696**, 3106–3112.

Kocyigit, O., Kursunlu, A. N. & Guler, E. (2010). *J. Hazard. Mater.* **183**, 334–340.

McKinnon, J. J., Spackman, M. A. & Mitchell, A. S. (2004). *Acta Cryst.* B**60**, 627–668.

Sheldrick, G. M. (2008). *Acta Cryst.* A**64**, 112–122.

Simonsen, J. B. (2010). *Surf. Sci.* **604**, 1300–1309.

Spitler, E. L., Koo, B. T., Novotney, J. L., Colson, J. W., Uribe-Romo, F. J., Gutierrez, G. D., Clancy, P. & Dichtel, W. R. (2011). *J. Am. Chem. Soc.* **133**, 19416–19421.

Thébault, F., Öhrström, L. & Haukka, M. (2011). *Acta Cryst.* C**67**, o143–o145.

Toda, F., Tanaka, K., Matsumoto, T., Nakai, T., Miyahara, I. & Hirotsu, K. (2000). *J. Phys. Org. Chem.* **13**, 39–45.

Waldvogel, S. R., Fröhlich, R. & Schalley, C. A. (2000). *Angew. Chem. Int. Ed.* **39**, 2472–24755.

Wallentin, C. J., Orentas, E., Johnson, M. T., Bathori, N. B., Butkus, E., Wendt, O. F., Wärnmark, K. & Öhrström, L. (2012). *CrystEngComm*, **14**, 178–187.

Wallentin, C.-J., Orentas, E., Johnson, M. T., Butkus, E., Wendt, O., Öhrström, L. & Wärnmark, K. (2009). *CrystEngComm*, **11**, 1837–1841.

Wells, A. F. (1954). *Acta Cryst.* **7**, 842–848.

Westrip, S. P. (2010). *J. Appl. Cryst.* **43**, 920–925.

Zniber, R., Achour, R., Cherkaoui, M. Z., Donnio, B., Gehringer, L. & Guillon, D. (2002). *J. Mater. Chem.* **12**, 2208–2213.

A new methanol solvate and Hirshfeld analysis of π-stacking in 2,3,6,7,10,11-hexahydroxytriphenylene solvates

Anirban Karmakar, Ana E. Platero-Prats and Lars Öhrström

2,3,6,7,10,11-Hexahydroxytriphenylene methanol monosolvate

Crystal data

$C_{18}H_{12}O_6 \cdot CH_4O$	$Z = 2$
$M_r = 356.32$	$F(000) = 372$
Triclinic, $P\bar{1}$	$D_x = 1.560$ Mg m^{-3}
Hall symbol: -P 1	Mo $K\alpha$ radiation, $\lambda = 0.71073$ Å
$a = 7.5894$ (7) Å	Cell parameters from 1226 reflections
$b = 10.550$ (1) Å	$\theta = 3.4–28.8°$
$c = 11.238$ (2) Å	$\mu = 0.12$ mm^{-1}
$\alpha = 62.88$ (1)°	$T = 293$ K
$\beta = 71.89$ (1)°	Prismatic, colourless
$\gamma = 77.782$ (9)°	$0.15 \times 0.10 \times 0.10$ mm
$V = 758.6$ (2) Å^3	

Data collection

Agilent Xcalibur Sapphire3 diffractometer	2683 independent reflections
Radiation source: fine-focus sealed tube	1613 reflections with $I > 2\sigma(I)$
Graphite monochromator	$R_{int} = 0.032$
Detector resolution: 16.5467 pixels mm^{-1}	$\theta_{max} = 25.0°$, $\theta_{min} = 3.4°$
ω scans	$h = -9 \rightarrow 8$
4609 measured reflections	$k = -12 \rightarrow 10$
	$l = -13 \rightarrow 8$

Refinement

Refinement on F^2	Secondary atom site location: difference Fourier map
Least-squares matrix: full	
$R[F^2 > 2\sigma(F^2)] = 0.053$	Hydrogen site location: inferred from neighbouring sites
$wR(F^2) = 0.114$	
$S = 0.97$	H atoms treated by a mixture of independent and constrained refinement
2673 reflections	
255 parameters	$w = 1/[\sigma^2(F_o^2) + (0.0272P)^2]$
0 restraints	where $P = (F_o^2 + 2F_c^2)/3$
Primary atom site location: structure-invariant direct methods	$(\Delta/\sigma)_{max} < 0.001$
	$\Delta\rho_{max} = 0.22$ e Å^{-3}
	$\Delta\rho_{min} = -0.23$ e Å^{-3}

Special details

Geometry. All esds (except the esd in the dihedral angle between two l.s. planes) are estimated using the full covariance matrix. The cell esds are taken into account individually in the estimation of esds in distances, angles and torsion angles; correlations between esds in cell parameters are only used when they are defined by crystal symmetry. An approximate (isotropic) treatment of cell esds is used for estimating esds involving l.s. planes.

Refinement. Refinement of F^2 against ALL reflections. The weighted R-factor wR and goodness of fit S are based on F^2, conventional R-factors R are based on F, with F set to zero for negative F^2. The threshold expression of $F^2 > 2sigma(F^2)$ is used only for calculating R-factors(gt) etc. and is not relevant to the choice of reflections for refinement. R-factors based on F^2 are statistically about twice as large as those based on F, and R- factors based on ALL data will be even larger.

Fractional atomic coordinates and isotropic or equivalent isotropic displacement parameters ($Å^2$)

	x	y	z	$U_{iso}*/U_{eq}$
C1	0.3146 (3)	0.7214 (3)	0.2703 (2)	0.0239 (6)
C2	0.3288 (3)	0.8232 (3)	0.1359 (3)	0.0275 (7)
C3	0.4466 (3)	0.7925 (3)	0.0299 (2)	0.0284 (7)
H3	0.4571	0.8611	−0.0604	0.034*
C4	0.5514 (3)	0.6605 (3)	0.0547 (2)	0.0231 (6)
C5	0.5359 (3)	0.5573 (3)	0.1910 (2)	0.0228 (6)
C6	0.4140 (3)	0.5916 (3)	0.2982 (2)	0.0252 (6)
H6	0.4014	0.5246	0.3892	0.030*
C7	0.6753 (3)	0.6292 (3)	−0.0595 (2)	0.0216 (6)
C8	0.6914 (3)	0.7293 (3)	−0.1974 (2)	0.0271 (7)
H8	0.6223	0.8173	−0.2161	0.033*
C9	0.8055 (3)	0.7008 (3)	−0.3045 (2)	0.0267 (7)
C10	0.9118 (3)	0.5704 (3)	−0.2788 (2)	0.0259 (6)
C11	0.8989 (3)	0.4713 (3)	−0.1463 (2)	0.0259 (6)
H11	0.9701	0.3844	−0.1299	0.031*
C12	0.7807 (3)	0.4964 (3)	−0.0330 (2)	0.0216 (6)
C13	0.6441 (3)	0.4192 (3)	0.2191 (2)	0.0217 (6)
C14	0.7650 (3)	0.3904 (3)	0.1080 (2)	0.0224 (6)
C15	0.8691 (3)	0.2565 (3)	0.1398 (2)	0.0283 (7)
H15	0.9477	0.2350	0.0682	0.034*
C16	0.8577 (3)	0.1580 (3)	0.2720 (2)	0.0282 (7)
C17	0.7369 (3)	0.1865 (3)	0.3810 (2)	0.0264 (7)
C18	0.6328 (3)	0.3143 (3)	0.3536 (2)	0.0250 (6)
H18	0.5518	0.3322	0.4267	0.030*
C19	0.2436 (4)	0.1776 (4)	0.7644 (3)	0.0634 (11)
H19A	0.2889	0.2103	0.8155	0.095*
H19B	0.3354	0.1103	0.7391	0.095*
H19C	0.1308	0.1322	0.8204	0.095*
O1	0.1978 (2)	0.7616 (2)	0.37271 (17)	0.0344 (5)
H1A	0.153 (4)	0.692 (3)	0.442 (3)	0.052*
O2	0.2335 (3)	0.9551 (2)	0.10383 (19)	0.0490 (7)
H2A	0.169 (4)	0.958 (4)	0.173 (3)	0.073*
O9	0.8190 (3)	0.7971 (2)	−0.43977 (17)	0.0400 (6)
H9A	0.762 (4)	0.878 (3)	−0.448 (3)	0.060*
O10	1.0239 (2)	0.5496 (2)	−0.39215 (17)	0.0363 (6)
H10A	1.078 (4)	0.465 (3)	−0.368 (3)	0.054*
O16	0.9705 (3)	0.0325 (2)	0.29697 (18)	0.0418 (6)

H16A	0.958 (4)	−0.024 (3)	0.381 (3)	0.063*
O17	0.7298 (3)	0.0807 (2)	0.51404 (19)	0.0392 (6)
H17A	0.739 (4)	0.124 (4)	0.556 (3)	0.059*
O19	0.2076 (3)	0.2963 (2)	0.6428 (2)	0.0571 (7)
H19	0.1792	0.2675	0.5953	0.086*

Atomic displacement parameters (Å²)

	U^{11}	U^{22}	U^{33}	U^{12}	U^{13}	U^{23}
C1	0.0267 (14)	0.0237 (16)	0.0193 (13)	−0.0005 (11)	0.0013 (11)	−0.0124 (12)
C2	0.0293 (15)	0.0217 (16)	0.0244 (15)	0.0061 (12)	−0.0043 (12)	−0.0085 (12)
C3	0.0339 (15)	0.0270 (17)	0.0168 (13)	0.0020 (12)	−0.0023 (12)	−0.0074 (12)
C4	0.0241 (14)	0.0244 (16)	0.0189 (13)	0.0000 (11)	−0.0037 (11)	−0.0093 (12)
C5	0.0214 (13)	0.0253 (16)	0.0183 (13)	−0.0027 (11)	−0.0023 (11)	−0.0076 (12)
C6	0.0303 (14)	0.0229 (16)	0.0171 (13)	0.0025 (12)	−0.0033 (11)	−0.0076 (11)
C7	0.0211 (13)	0.0215 (15)	0.0208 (13)	−0.0012 (11)	−0.0023 (11)	−0.0097 (12)
C8	0.0297 (14)	0.0219 (16)	0.0259 (15)	0.0020 (11)	−0.0032 (12)	−0.0110 (12)
C9	0.0304 (15)	0.0254 (16)	0.0180 (14)	−0.0012 (12)	−0.0032 (11)	−0.0059 (12)
C10	0.0287 (14)	0.0294 (17)	0.0203 (14)	−0.0028 (12)	0.0006 (11)	−0.0150 (12)
C11	0.0287 (14)	0.0230 (16)	0.0239 (14)	0.0010 (11)	−0.0050 (12)	−0.0104 (12)
C12	0.0214 (13)	0.0238 (16)	0.0190 (13)	−0.0020 (11)	−0.0016 (11)	−0.0106 (11)
C13	0.0256 (14)	0.0200 (15)	0.0194 (13)	−0.0017 (11)	−0.0052 (11)	−0.0085 (11)
C14	0.0244 (14)	0.0235 (15)	0.0198 (13)	−0.0006 (11)	−0.0057 (11)	−0.0099 (12)
C15	0.0336 (15)	0.0289 (17)	0.0201 (14)	0.0025 (12)	−0.0021 (11)	−0.0135 (12)
C16	0.0332 (15)	0.0217 (16)	0.0252 (15)	0.0058 (12)	−0.0070 (12)	−0.0098 (12)
C17	0.0358 (15)	0.0231 (16)	0.0162 (13)	0.0018 (12)	−0.0058 (11)	−0.0070 (12)
C18	0.0304 (15)	0.0230 (16)	0.0199 (14)	0.0013 (12)	−0.0016 (11)	−0.0118 (12)
C19	0.070 (2)	0.054 (3)	0.073 (3)	0.0022 (19)	−0.033 (2)	−0.026 (2)
O1	0.0467 (12)	0.0274 (12)	0.0180 (10)	0.0062 (9)	0.0019 (9)	−0.0105 (8)
O2	0.0601 (14)	0.0326 (13)	0.0299 (12)	0.0203 (11)	0.0014 (10)	−0.0108 (10)
O9	0.0579 (14)	0.0293 (13)	0.0174 (10)	0.0066 (10)	−0.0011 (9)	−0.0065 (9)
O10	0.0497 (13)	0.0282 (12)	0.0209 (10)	0.0030 (9)	0.0044 (9)	−0.0128 (9)
O16	0.0572 (13)	0.0278 (13)	0.0245 (10)	0.0165 (10)	−0.0051 (10)	−0.0094 (9)
O17	0.0667 (13)	0.0240 (12)	0.0197 (11)	0.0066 (10)	−0.0094 (9)	−0.0082 (9)
O19	0.0813 (16)	0.0464 (16)	0.0557 (15)	0.0184 (12)	−0.0336 (12)	−0.0309 (12)

Geometric parameters (Å, º)

C1—C6	1.364 (3)	C13—C18	1.397 (3)
C1—C2	1.383 (3)	C13—C14	1.417 (3)
C1—O1	1.393 (3)	C14—C15	1.411 (3)
C1—O1	1.393 (3)	C15—C16	1.359 (3)
C2—O2	1.367 (3)	C15—H15	0.9300
C2—C3	1.375 (3)	C16—O16	1.377 (3)
C3—C4	1.402 (3)	C16—C17	1.397 (3)
C3—H3	0.9300	C17—C18	1.364 (3)
C4—C5	1.403 (3)	C17—O17	1.393 (3)
C4—C7	1.465 (3)	C17—O17	1.393 (3)
C5—C6	1.414 (3)	C18—H18	0.9300
C5—C13	1.460 (3)	C19—O19	1.427 (3)

C6—H6	0.9300	C19—H19A	0.9600
C7—C8	1.406 (3)	C19—H19B	0.9600
C7—C12	1.408 (3)	C19—H19C	0.9600
C8—C9	1.364 (3)	O1—O1	0.000 (6)
C8—H8	0.9300	O1—H1A	0.83 (3)
C9—O9	1.375 (3)	O2—H2A	0.79 (3)
C9—C10	1.393 (3)	O9—H9A	0.85 (3)
C10—C11	1.361 (3)	O10—H10A	0.86 (3)
C10—O10	1.377 (3)	O16—H16A	0.84 (3)
C11—C12	1.412 (3)	O17—O17	0.000 (9)
C11—H11	0.9300	O17—H17A	0.81 (4)
C12—C14	1.450 (3)	O19—H19	0.8200
C6—C1—C2	120.9 (2)	C18—C13—C14	118.8 (2)
C6—C1—O1	123.1 (2)	C18—C13—C5	121.5 (2)
C2—C1—O1	116.0 (2)	C14—C13—C5	119.7 (2)
C6—C1—O1	123.1 (2)	C15—C14—C13	117.8 (2)
C2—C1—O1	116.0 (2)	C15—C14—C12	121.7 (2)
O1—C1—O1	0.00 (15)	C13—C14—C12	120.5 (2)
O2—C2—C3	118.2 (2)	C16—C15—C14	121.8 (2)
O2—C2—C1	122.7 (2)	C16—C15—H15	119.1
C3—C2—C1	119.0 (2)	C14—C15—H15	119.1
C2—C3—C4	121.6 (2)	C15—C16—O16	119.2 (2)
C2—C3—H3	119.2	C15—C16—C17	120.0 (2)
C4—C3—H3	119.2	O16—C16—C17	120.7 (2)
C3—C4—C5	119.2 (2)	C18—C17—O17	123.1 (2)
C3—C4—C7	120.9 (2)	C18—C17—O17	123.1 (2)
C5—C4—C7	119.9 (2)	O17—C17—O17	0.0 (3)
C4—C5—C6	118.1 (2)	C18—C17—C16	119.6 (2)
C4—C5—C13	120.1 (2)	O17—C17—C16	117.3 (2)
C6—C5—C13	121.9 (2)	O17—C17—C16	117.3 (2)
C1—C6—C5	121.2 (2)	C17—C18—C13	121.9 (2)
C1—C6—H6	119.4	C17—C18—H18	119.0
C5—C6—H6	119.4	C13—C18—H18	119.0
C8—C7—C12	118.4 (2)	O19—C19—H19A	109.5
C8—C7—C4	121.3 (2)	O19—C19—H19B	109.5
C12—C7—C4	120.3 (2)	H19A—C19—H19B	109.5
C9—C8—C7	121.8 (2)	O19—C19—H19C	109.5
C9—C8—H8	119.1	H19A—C19—H19C	109.5
C7—C8—H8	119.1	H19B—C19—H19C	109.5
C8—C9—O9	122.1 (2)	O1—O1—C1	0 (10)
C8—C9—C10	120.1 (2)	O1—O1—H1A	0 (10)
O9—C9—C10	117.9 (2)	C1—O1—H1A	111 (2)
C11—C10—O10	123.9 (2)	C2—O2—H2A	108 (2)
C11—C10—C9	119.5 (2)	C9—O9—H9A	113 (2)
O10—C10—C9	116.7 (2)	C10—O10—H10A	111 (2)
C10—C11—C12	122.0 (2)	C16—O16—H16A	115 (2)
C10—C11—H11	119.0	O17—O17—C17	0 (10)
C12—C11—H11	119.0	O17—O17—H17A	0 (10)

C7—C12—C11	118.3 (2)	C17—O17—H17A	103 (2)
C7—C12—C14	119.6 (2)	C19—O19—H19	109.5
C11—C12—C14	122.1 (2)		
C6—C1—C2—O2	−179.1 (3)	C8—C7—C12—C14	−179.2 (2)
O1—C1—C2—O2	−0.7 (4)	C4—C7—C12—C14	0.4 (4)
O1—C1—C2—O2	−0.7 (4)	C10—C11—C12—C7	−0.7 (4)
C6—C1—C2—C3	−0.7 (4)	C10—C11—C12—C14	179.2 (3)
O1—C1—C2—C3	177.8 (2)	C4—C5—C13—C18	179.7 (3)
O1—C1—C2—C3	177.8 (2)	C6—C5—C13—C18	−0.2 (4)
O2—C2—C3—C4	179.0 (3)	C4—C5—C13—C14	0.2 (4)
C1—C2—C3—C4	0.5 (4)	C6—C5—C13—C14	−179.7 (3)
C2—C3—C4—C5	−0.2 (4)	C18—C13—C14—C15	−0.4 (4)
C2—C3—C4—C7	179.6 (3)	C5—C13—C14—C15	179.1 (2)
C3—C4—C5—C6	0.0 (4)	C18—C13—C14—C12	180.0 (2)
C7—C4—C5—C6	−179.7 (2)	C5—C13—C14—C12	−0.5 (4)
C3—C4—C5—C13	−179.8 (2)	C7—C12—C14—C15	−179.4 (3)
C7—C4—C5—C13	0.4 (4)	C11—C12—C14—C15	0.7 (4)
C2—C1—C6—C5	0.6 (4)	C7—C12—C14—C13	0.2 (4)
O1—C1—C6—C5	−177.8 (2)	C11—C12—C14—C13	−179.7 (3)
O1—C1—C6—C5	−177.8 (2)	C13—C14—C15—C16	−1.0 (4)
C4—C5—C6—C1	−0.2 (4)	C12—C14—C15—C16	178.6 (3)
C13—C5—C6—C1	179.6 (2)	C14—C15—C16—O16	−176.3 (3)
C3—C4—C7—C8	−0.9 (4)	C14—C15—C16—C17	1.7 (4)
C5—C4—C7—C8	178.8 (3)	C15—C16—C17—C18	−0.9 (4)
C3—C4—C7—C12	179.5 (2)	O16—C16—C17—C18	177.1 (3)
C5—C4—C7—C12	−0.7 (4)	C15—C16—C17—O17	179.2 (3)
C12—C7—C8—C9	−0.1 (4)	O16—C16—C17—O17	−2.8 (4)
C4—C7—C8—C9	−179.6 (3)	C15—C16—C17—O17	179.2 (3)
C7—C8—C9—O9	178.6 (3)	O16—C16—C17—O17	−2.8 (4)
C7—C8—C9—C10	−0.7 (4)	O17—C17—C18—C13	179.3 (3)
C8—C9—C10—C11	0.8 (4)	O17—C17—C18—C13	179.3 (3)
O9—C9—C10—C11	−178.6 (3)	C16—C17—C18—C13	−0.6 (4)
C8—C9—C10—O10	−179.9 (3)	C14—C13—C18—C17	1.2 (4)
O9—C9—C10—O10	0.7 (4)	C5—C13—C18—C17	−178.3 (3)
O10—C10—C11—C12	−179.3 (3)	C6—C1—O1—O1	0.0 (2)
C9—C10—C11—C12	−0.1 (4)	C2—C1—O1—O1	0.00 (18)
C8—C7—C12—C11	0.8 (4)	C18—C17—O17—O17	0.00 (9)
C4—C7—C12—C11	−179.7 (2)	C16—C17—O17—O17	0.00 (12)

Hydrogen-bond geometry (Å, º)

D—H⋯A	D—H	H⋯A	D⋯A	D—H⋯A
O16—H16A⋯O17	0.84 (3)	2.35 (3)	2.741 (3)	109 (2)
O9—H9A⋯O17[i]	0.85 (3)	1.96 (3)	2.761 (3)	158 (3)
O17—H17A⋯O1[ii]	0.81 (4)	1.93 (4)	2.729 (3)	170 (3)
O10—H10A⋯O19[iii]	0.86 (3)	1.81 (3)	2.655 (3)	168 (3)
O2—H2A⋯O1	0.79 (3)	2.29 (3)	2.734 (3)	116 (3)
O2—H2A⋯O16[iv]	0.79 (3)	2.00 (3)	2.756 (2)	159 (3)

O1—H1A···O10^v	0.83 (3)	1.90 (3)	2.724 (3)	172 (3)
O19—H19···O9^{vi}	0.82 (4)	2.14 (4)	2.939 (3)	164 (4)

Symmetry codes: (i) x, $y+1$, $z-1$; (ii) $-x+1$, $-y+1$, $-z+1$; (iii) $x+1$, y, $z-1$; (iv) $x-1$, $y+1$, z; (v) $x-1$, y, $z+1$; (vi) $-x+1$, $-y+1$, $-z+2$.